Highlights

-Caged Ang-II shows lower affinity towards AT1R and AT2R.

-Caged Ang-II is more cell-permeable than Ang-II

-Caged Ang-II allows selective activation of nuclear ATRs.

-Nuclear ATR activation produces a greater change in $[Ca^{2+}]_n$ that cell surface ATRs.

Caged Ligands to Study the Role of Intracellular GPCRs

Artavazd Tadevosyan[a,b], Louis R Villeneuve[b], Alain Fournier[c,d], David Chatenet[c,d], Stanley Nattel[a,b,e] Bruce G Allen[a,b,e,f]

[a]Department of Medicine, Université de Montréal, [b]Montreal Heart Institute, [c]INRS–Institut Armand-Frappier, Université du Québec, [d]Laboratoire International Associé Samuel de Champlain, [e]Department of Pharmacology and Therapeutics, McGill University, [f]Department of Biochemistry and Molecular Medicine, Université de Montréal.

Running title: Assessing the role of intracellular GPCRs

Correspondence to:
Stanley Nattel OR Bruce G. Allen, 5000 Bélanger St., Montréal, Québec, H1T 1C8, Canada. Tel.: (514)-376-3330; Fax: (514)-376-1355; E-mail: bruce.g.allen@umontreal.ca **OR** stanley.nattel@icm-mhi.org

Abstract

In addition to cell surface membranes, numerous G protein-coupled receptors (GPCRs) are located on intracellular membranes including the nuclear envelope. Although the role of numerous GPCRs at the cell surface has been well characterized, the physiological function of these same receptors located on intracellular membranes remains to be determined. Here, we employ a novel caged Ang-II analog, cAng-II, to compare the effects of the activation of cell surface versus intracellular angiotensin receptors in intact cardiomyocytes. When added extracellularly to HEK 293 cells, Ang-II and photolysed cAng-II increased ERK1/2 phosphorylation (via AT1R) and cGMP production (AT2R). In contrast unphotolysed cAng-II did not. Cellular uptake of cAng-II was 6-fold greater than that of Ang-II and comparable to the HIV TAT(48-60) peptide. Intracellular photolysis of cAng-II induced an increase in nucleoplasmic Ca^{2+} ($[Ca^{2+}]_n$) that was greater than that induced by extracellular application of Ang-II. We conclude that cell-permeable ligands that can access intracellular GPCRs may evoke responses distinct from those with access restricted to the same receptor located on the cell surface.

Keywords: Intracrine signalling, Angiotensin II, Angiotensin receptors, nuclear GPCR, live cell imaging

Abbreviations: AT1R, angiotensin II type 1 receptor; AT2R, angiotensin II type 2 receptor; ACE, angiotensin-converting enzyme; DMNB, 4,5-dimethoxy-2-nitrobenzyl group; PACAP(28-38), peptide corresponding to amino acids 28-38 of the pituitary adenylyl cyclase-activating polypeptide; TAT(48-60), peptide corresponding to amino acids 48-60 of the HIV-1 TAT protein; UV, ultraviolet.

1. Introduction

Originally thought to functioning as simple on-off switches that are activated upon ligand binding, the biology of G protein-coupled receptors (GPCRs) is now known to be much more elaborate. GPCRs are now known to couple to various effector molecules in a ligand-dependent manner. This process is currently referred to as biased ligand signalling and provides additional insight into the complex and dynamic nature of GPCR signalling. To date, most models consider the receptor to be located on cell surface membranes when ligand binding initiates signalling. However, numerous GPCRs have been shown to localize to intracellular membranes such as nuclear and mitochondrial membranes in different primary cell systems, including cardiac myocytes, endothelial cells, vascular smooth muscle cells, neurons, hepatocytes, and kidney cells [1-3]. Intracellular GPCR signalling adds yet more complexity and selectivity to the system, as 1) a GPCR located on an intracellular membrane may serve a role that is distinct from the same receptor located at the cell surface and 2) there maybe be restrictions on which ligands can access its intracellular versus cell-surface receptor.

To access intracellular receptors, ligands must enter the cell. However, the nuclear envelope comprises a double bilayer, comprising the inner (INM) and outer nuclear membranes (ONM), the lumen of which is referred to as the perinuclear space or nuclear cisternae. Based on their biosynthesis and trafficking, GPCRs are likely oriented in the nuclear membrane with their ligand-binding site facing into the perinuclear space and their effector-binding domains facing either the cytosol or the interior of the nucleus. Hence, ligands must access the perinuclear space in order to reach their binding site on nuclear GPCRs. Hydrophobic ligands, such as prostaglandins, can cross membranes to access intracellular receptors. However, hydrophilic ligands require the presence of some form of active or passive transport mechanism in order to cross both the plasma and nuclear membranes. Ligand-mediated receptor internalization and translocation to the nucleus has been demonstrated for AT_1 [4]. In contrast, PGE_2 and catecholamines are taken up by specific transporters [5-7]. In both neonatal and adult

cardiomyocytes, the effects of extracellular phenylephrine are mediated, in part, by intracellular α_1AR [7-9] and extracellularly applied [^{3}H]norepinephrine accumulates within the nuclei of neonatal ventricular cardiomyocytes [10]. Hence, hydrophobic ligands that are able to cross the plasma membrane may show no selectivity for activating cell surface or intracellular signalling. Catecholamines, for example, can cross both the plasma membrane and nuclear membranes, thus having free access to both cell surface and nuclear receptors, in ventricular myocytes via the extraneuronal monoamine transporter (EMT/OCT3) [6]. In contrast, at least in cardiac cells, extracellular peptidergic ligands such as endothelin-1 and angiotensin II do not appear to be able to access intracellular receptors. In the case of Ang-II, numerous labs have demonstrated the presence of an intracellular renin-angiotensin system (RAS) that allows for the intracellular production of Ang-II.

Several approaches can be employed to activate intracellular receptors in intact cells. For example, cell-permeable ligands, in conjunction with impermeable antagonists to block cell-surface receptors [7]. In the case of peptidergic agonists, molecular approaches can be employed to increase intracellular ligand levels. However, these approaches would be more suited to observe slow changes, such as morphology. To obtain a degree of spatial and temporal resolution, or when using ligands with poor cell permeability, biologically active molecules can be pressure-injected [11] or modified by the incorporation of a "caging" moiety [12]: an easily removable functional group that both increases cell permeability and reduces affinity of the ligand for its cognate binding site. This approach has been used to study the actions of a range of molecules, including ATP [13], GTP [14], endothelin-1, [15, 16], isoproterenol [17, 18], phenylephrine [19], γ-aminobutyric acid [20], urotensin II [21], endothelin receptor antagonists [16], IP_3 [22, 23], cofilin [24], DNA [25] and RNA [26, 27] in intact cells. Caged ligands can be introduced, uncaged with ultraviolet (UV) light, and the results assessed in either single cells or populations of cells. This permits the simultaneous study of the consequence of activating the

same GPCR when located at the cell surface versus the nuclear, or other intracellular, membrane in any primary cell type.

2. Materials and Methods

2.1. Synthesis and Purification of Caged Angiotensin-II

[Tyr(DMNB)^4]Ang-II **(**caged Ang-II; cAng-II), as well as fluorescein-conjugated derivatives of Ang-II, [Tyr(DMNB)^4]Ang-II, TAT(48-60), and PACAP(28-38) (e.g., fluorescein-[Ahx^0]Ang-II, fluorescein-[Ahx^0,Tyr(DMNB)^4]Ang-II, fluorescein-[Ahx^0]PACAP(28-38) or fluorescein-[Ahx^0]TAT(48-60)), were synthesized, purified, and validated as described previously [28].

2.2. Cell Culture and AT1R/AT2R Transfection

Human embryonic kidney 293 (HEK 293) cells were cultured in Dulbecco's modified Eagle's medium (DMEM) supplemented with 10% fetal bovine serum (FBS), 100 µg/ml streptomycin, 100 units/ml penicillin, and 2 mM L-glutamine at 37 °C in a humidified 5% CO_2-containing atmosphere. HEK 293 cells were seeded at a density of 4×10^4 cells per 20 mm well of 24-well plates, 1 x 10^5 cells per 35 mm well of 6-well plates, or 10^6 cells per 100 mm culture dish. For transient expression, expression vectors encoding AT1R-Venus or AT2R-Venus were transfected into in HEK 293 cells using polyethylenimine (PEI) at a final concentration of 9 µg/ml [29]. Assays were carried out 48 h after transfection.

2.3. ERK1/2 Phosphorylation

HEK 293 cells seeded in uncoated 6-well plates were transfected with either AT1R-Venus or AT2R-Venus as described above. Cells were serum-starved for 24 h prior to stimulation. On the day of the experiment, cells were washed twice with serum-free DMEM and the assay was initiated by adding the indicated ligands and incubated at 37 °C. To terminate the incubation, cells were placed on ice, the medium was removed, and then cells were washed twice with ice-

cold PBS. They were then scraped into ice-cold lysis buffer (25 mM Na-HEPES (pH 7.4), 150 mM NaCl, 25 mM NaF, 10 mM $MgCl_2$, 1 mM EGTA, 1 mM Na_3VO_4, 0.025% sodium deoxycholate, 10% glycerol (v/v), 10 μg/ml leupeptin, 10 μM benzamidine, 0.5 μM microcystin LR, 1% Triton X-100 (v/v), 0.1 mM phenylmethylsulfonyl fluoride and 5 mM dithiothreitol). After incubating on ice for 30 min, lysates were cleared by centrifugation at 10000 ×g for 10 min, and the supernatants retained. The protein concentration of each lysate was determined, before being denatured using Laemmli sample buffer, and resolved by electrophoresis on SDS-polyacrylamide gels (SDS-PAGE, 10% acrylamide gels). Proteins were transferred onto polyvinylidene difluoride membranes, probed with a phospho-ERK1/2-specific antibody (Cell Signaling Technology) and then, after stripping the membranes with Re-blot Plus mild antibody stripping solution (Millipore), re-probed using an ERK1/2-specific antibody (Abcam) to assess the total ERK immunoreactivity. Horseradish peroxidase-conjugated secondary antibodies (Jackson ImmunoResearch Inc.) were used and immunoreactive bands were revealed by chemiluminescence and quantified using the Quantity One 1-D analysis software (Bio-Rad Laboratories).

2.4. Live-Cell Fluorescence Imaging

To assess the cell permeability of cAng-II, fluorescein-conjugated derivatives of Ang-II, cAng-II, TAT(48-60), and PACAP(28-38) were synthesized and accumulation of fluorescein-conjugated peptides in HEK 293 cells examined. HEK 293 cells (non-transfected) were grown on glass coverslips, incubated for 60 min at 37 °C with the fluorescent peptide in HEPES-Krebs-Ringer (HKR) buffer (5 mM HEPES, 2.68 mM KCl, 137 mM NaCl, 2.05 mM $MgCl_2$, 1.8 mM $CaCl_2$ and 1 g/l glucose, pH 7.4), washed extensively, and then incubated for 5 min with Cell Mask (1:1000; Invitrogen) and DRAQ5 (1:1000; BioStatus) to label the plasma membrane and nucleus, respectively. Fluorescence was then visualized with an Olympus FluoView FV1000 inverted confocal microscope. Separate channels were employed for each fluorophore (*i.e.* FITC,

Cell Mask, DRAQ5) and the emission channels scanned sequentially to minimize crosstalk between overlapping emission spectra. Cells were imaged by serial z-stack progressive scans, background fluorescence subtracted, and fluorescence values quantified using FluoView Software (FV10-ASW).

To visualize changes in the nucleoplasmic Ca^{2+} concentration ($[Ca^{2+}]_n$), freshly isolated canine ventricular cardiomyocytes were plated at 37 °C for 60 min on laminin-coated 35 mm glass bottom culture dishes in Tyrode's physiological buffer. Cells were loaded with 5 μM Fluo-4AM (Invitrogen; from a 2.5 mM Fluo-4AM/10% Pluronic F125/DMSO stock) for 30 min in 10 mM HEPES (pH 7.4), 134 mM NaCl, 6 mM KCl, 10 mM glucose, 2 mM $CaCl_2$, 1 mM $MgCl_2$, and in the absence or presence of cAng-II, as described previously [16]. Cardiomyocytes were washed three times, stained with a live-cell-permeant DNA dye (DRAQ5; 1 μM) and used for Ca^{2+} imaging within 1 h. Images were obtained using a Zeiss LSM 7 Duo microscope (combined LSM710 and Zeiss Live systems) with a 63x/1.4 oil Plan-Apochromat objective. Fluo-4AM was excited using a 488-nm/100 mW diode (1-5% laser intensity) and fluorescence emitted between 495 nm and 550 nm was collected. Cells were scanned at 30 fps in bi-directional mode. The pixel size was set at 0.2 μm and the pinhole at 1.5 Airy units. After establishing a baseline, cAng-II was photolysed by a 70-mW pulse of UV-light using a 405-nm/30 mW diode. The power output from the 405-nm diode was measured at the level of the stage using an EC Plan-Neofluar 10x/0.3 objective lens using an X-Cite XR2100 optical power measurement system (Lumen Dynamics Group Inc.). DRAQ5 emissions were used to focus the UV-laser into a 60-μm^2 rectangular region overlapping the nucleus. The microscope stage (Zeiss Observer Z1) was equipped with a BC 405/561 dichroic mirror that permitted simultaneous photolysis of cAng-II (LSM 710 405 nm laser) and image acquisition (Zeiss Live). Intranuclear Ca^{2+} levels were expressed as a percentage of Fluo-4 fluorescence intensity relative to basal fluorescence ($\Delta[Ca^{2+}]Nuc(F/F_0;\%)$); basal fluorescence is the fluorescence intensity acquired 1 s prior to uncaging the cAng-II.

2.5. Canine Cardiomyocyte Isolation

Cardiac cell isolation was performed by perfusion with Tyrode's solution containing collagenase (100 U/mL, Worthington, type II) as previously described [30].

2.6. Statistical Analysis

Data are from a minimum of 3 independent experiments and are presented as mean ± SEM. Student's *t*-tests (for single 2-group comparisons) , 1-way or 2-way ANOVA with Bonferroni post hoc test (multiple groups with a common control) were used for statistical comparisons and $P<0.05$ or less was considered to be statistically significant. Analyses were performed using Prism version 6.0f for Mac OS X (GraphPad Software, La Jolla California USA)

3. Results

3.1. Synthesis of a Photoactivable Caged Ang-II Analog

To permit acute activation of intracellular angiotensin receptors in intact primary cardiac cells, without activating the angiotensin receptors at the cell surface, a caged analog of Ang-II was synthesized. A photo-labile 4,5-dimethoxy-2-nitrobenzyl (DMNB) group was incorporated onto the aromatic side chain of tyrosine-4 as described previously [12, 28]. To be of use in studying signalling in intact cells, a caged Ang-II (cAng-II) analog must possess the following characteristics (relative to unmodified Ang-II): 1) reduced affinity and efficacy for ATR1 and ATR2 activation, 2) increased cell permeability, 3) release of the active form of the ligand upon uncaging.

3.2. Characterization of the cAng-II

The inability of the caged Ang-II analog (in the absence of uncaging) to activate cell-surface angiotensin receptors was evaluated in HEK293 cells expressing recombinant AT1R or AT2R. AT1R-stimulation activates the ERK1/2 MAP kinase cascade. Hence, to assess the effects of caging Ang-II upon its ability to activate AT1 receptors, we compared the ability of extracellular cAng-II and Ang-II to increase ERK1/2 phosphorylation in HEK 293 cells transiently transfected with AT1R. Whereas 10 nM Ang-II (5 min, 37 °C) increased ERK phosphorylation, 10 nM cAng-II did not (**Figure 1**). In fact, at concentrations up to 1 μM, cAng-II failed to alter ERK1/2 phosphorylation (not shown). In contrast, following photolysis, 10 nM cAng-II increased in ERK1/2 phosphorylation to levels comparable to that induced by Ang-II (**Figure 1**). UV-irradiation alone did not increase ERK1/2 phosphorylation. Consistent with being AT1R-mediated, both Ang-II-induced and photolysed-cAng-II-induced ERK

phosphorylation was inhibited by an AT1R antagonist, valsartan (**Figure 1**). Hence, cAng-II is unable to activate AT1R at concentrations as high as 1 μM.

AT2R couple to NO synthase and guanylate cyclase activation. Hence, to determine if caging Ang-II effectively reduced its ability to activate AT2 receptors, the effects of extracellular cAng-II and Ang-II on AT2R activation was assessed by measuring cGMP levels in HEK 293 cells transiently transfected with AT2R. cGMP production in Ang-II-treated cells (10 nM, 45 min) was 2-fold greater than vehicle-treated cells (**Figure 2**). In contrast, 10 nM cAng-II had no effect on the cGMP levels. Upon uncaging, 10 nM cAng-II increased the cellular cGMP content by 2-fold. UV irradiation alone had no effect. An AT2R-selective antagonist, PD 123319, prevented both Ang-II and photolysed-cAng-II from increasing cGMP levels. Similarly, preincubating HEK 293 cells with the non-selective NO synthase inhibitor L-NAME attenuated the increase in cGMP induced by both Ang-II and photolysed-cAng-II. Hence, at a concentration of 10 nM, cAng-II alone was unable to activate AT2R without prior photolysis.

3.3. Cell Permeability of cAng-II

In the context of studying intracellular receptor function, one of the requirements of the caging moiety is that it increases the ability of the ligand to access the interior of the cell. To test the ability of cAng-II to cross the plasma membrane, fluorescein-labeled derivatives of angiotensin-II (fluorescein-Ang-II) and its caged analogue (fluorescein-cAng-II) were synthesized. Untransfected HEK 293 cells, which do not express either AT1 or AT2 receptors, were employed, thus eliminating any uptake that may have resulted from endocytosis of receptor-ligand complexes. The uptake of fluorescein-Ang-II and fluorescein-cAng-II was compared to that of fluorescein TAT(48-60), a cell permeable peptide derived from the HIV transactivating regulatory protein TAT, and fluorescein-PACAP(28-38), an impermeant, highly basic segment of pituitary adenylyl cyclase-activating polypeptide [31]. Following incubation with the indicated fluorescein-conjugated peptide, cells were subjected to acidic washes to

remove peptides non-specifically bound to the extracellular surface, and peptide uptake was determined by confocal fluorescence microscopy. CellMask™ orange was used to delineate the plasma membrane. No increase in intracellular fluorescence over background was observed with fluorescein-PACAP(28-38). The intracellular fluorescence intensity of fluorescein-cAng-II was comparable to that of fluorescein-TAT(48-60) and 6-fold greater than that of fluorescein-Ang-II (**Figure 3**). Thus, cAng-II shows greatly enhanced cell permeability relative to Ang-II.

3.4. Cell surface and nuclear Ang-II receptors differ in their ability to regulate $[Ca^{2+}]_n$

cAng-II is cell permeable, unable to activate AT1R or AT2R at concentrations on the order of 10 nM, but regains its pharmacological activity upon photolysis with UV radiation. Hence, cAng-II is a suitable reagent to employ to compare the functional effects of activation of cell surface angiotensin receptors with these same receptors located on the nuclear membrane in intact cells. We have shown previously that Ang-II alters transcription and releases Ca^{2+} from perinuclear stores in nuclei isolated from adult hearts and adult cardiomyocytes [32]. Hence, we employed these two experimental endpoints to compare and contrast the effects of activating cell surface versus nuclear Ang-II receptors. In adult cardiomyocytes, photolysis of intracellular cAng-II produced increases in both NF-κB mRNA and 18S rRNA that were similar to those induce by addition of Ang-II to the extracellular media (not shown, [28]). Changes in $[Ca^{2+}]_n$ were visualized using the cell-permeable Ca^{2+} dye Fluo-4 AM. Following incubation in the presence of 20 nM cAng-II, cells were washed to remove any remaining extracellular cAng-II. Photolysis of intracellular cAng-II caused a significant increase in $[Ca^{2+}]_n$ whereas non-photolysed cAng-II did not (**Figure 4**). To verify that the response observed was not the result of Ang-II leaving the cells following photolysis and acting on cell surface receptors, where indicated, cells loaded with cAng-II were pre-treated for 20 min with, and photolysed in the presence of, the AT1R antagonist valsartan (1 μM). Extracellular valsartan did not reduce the magnitude of the increase in $[Ca^{2+}]_n$ induced upon photolysis of intracellular cAng-II.

Preincubation with the IP3R inhibitor 2-APB (100 μM), which completely blocks the Ang-II-evoked release of Ca^{2+} from perinuclear stores in nuclei isolated from cardiomyocytes [32], prevented the increase in $[Ca^{2+}]_n$ following photolysis of cAng-II. UV-irradiation of cardiomyocytes not loaded with cAng-II induced no change in $[Ca^{2+}]_n$. In contrast to intracellular release of Ang-II from cAng-II, extracellular application of 20 nM Ang-II caused an increase in $[Ca^{2+}]_n$ that was abolished when cells were pre-treated with valsartan (1 μM). Furthermore, the increase in $[Ca^{2+}]_n$ induced by extracellular Ang-II was significantly smaller in magnitude than that evoked by the uncaging of intracellular cAng-II. Hence, although activation of ATRs on the cell surface resulted in equivalent increases in the abundance of NF-κB mRNA and 18S rRNA, activation of ATRs on the nuclear membrane have a much more dramatic effect on $[Ca^{2+}]_n$. The physiological implications of this difference remain to be determined.

4. Discussion

The presence of functional Ang-II receptors on the nuclear membrane suggests that GPCR signalling may occur on intracellular membranes [33]. To study the role of nuclear Ang-II receptors and compare their signalling and physiological function with that of receptors at the cell surface we synthesized a caged Ang-II analog, [Tyr(DMNB)^4]Ang-II (cAng-II). cAng-II is cell permeable and inactive towards both AT1R and AT2R at nanomolar concentrations; however, cAng-II is converted back to active Ang-II upon irradiation with UV. We have shown that although activation of Ang-II receptors at the cell surface and nucleus produce similar increases in 18S rRNA and NF-κB mRNA in rat cardiomyocytes, photolysis of intracellular cAng-II resulted in larger increases in $[Ca^{2+}]_n$ than observed upon addition of Ang-II to the extracellular media. Hence, these two receptor populations are not functionally eqivalent.

Cardiomyocytes express angiotensinogen, angiotensin converting enzyme (ACE), and renin [34-36]. Thus, all of the components required for the production of Ang II are present within cardiomyocytes. In addition, there is evidence suggesting that intracellular Ang II (iAng II) is involved in cardiomyopathy. Ang-II immunoreactivity is increased 3-fold in cardiomyocytes and cardiac endothelial cells from patients with type 2 diabetes and a further 2-fold increase is detected in diabetic patients who are also hypertensive [37]. Elevated glucose increases iAng II in rat neonatal and adult cardiomyocytes [38, 39], fibroblasts [40], vascular smooth muscle cells (VSMC) [41], and mesangial cells [42]. Furthermore, cardiomyocyte-targeted overexpression of Ang-II or angiotensinogen in mice increases iAng-II and induces hypertrophy [43, 44]: this elevated iAng-II is not associated with increases in blood pressure or plasma Ang-II concentrations and the resulting hypertrophic effect is no prevented by the AT_1 antagonist losartan [43]. Hence, the chronic activation of intracrine Ang-II signalling may be sufficient to induce hypertrophy; however, the regulation of iAng-II biosynthesis and the means whereby it accesses nuclear ATRs are currently not well understood.

There may be cell-type differences in iAng-II signalling. A splice variant of renin lacking the secretion signal sequence has been demonstrated in rat heart: this variant would be expected to function exclusively within cardiac cells [36]. Similarly, as mentioned above, ACE immunoreactivity has been detected within the nuclei of rat cardiomyocytes, fibroblasts, and mesangial cells [45, 46]. It remains to be determined if Ang-II receptors are only found on the nuclear membrane in cells that are able to produce Ang-II endogenously. In cell types lacking the ability to produce iAng-II, the consequences of physiological or pathological conditions that alter iAng-II production may be negligible. Similarly, the function of a pharmacological agent may be modified by its ability to access intracellular receptors. The ability of phenylephrine to induce hypertrophy in neonatal cardiomyocytes is inhibited by a cell-permeable α-adrenoceptor antagonist but not by a cell-impermeable antagonist. Thus, the physiological function of nuclear GPCRs may be influenced by 1) the cell-types that traffic a particular receptor, or receptor subtype, to the nuclear membrane, 2) the presence of a mechanism whereby the ligand for the receptor can access its cognate ligand binding site when oriented towards the lumen of the nuclear envelope, and 3) the effector molecules coupled to, and regulated by, the cell surface and nuclear receptors. Furthermore, having taken these factors into consideration, a therapeutic agent may have markedly different pharmacological effects depending upon which population of receptors it is capable of accessing: a prodrug, analogous to a caged ligand, that is converted to its pharmacologically active form within the cell, may offer exciting new possibilities for therapeutic intervention in the case where the physiological function of the intracellular receptor is distinct from that of the same receptor, or receptor subtype, at the cell surface (**Table 1**).

5. Concluding Remarks

In summary, incorporating a photosensitive 4,5-dimethoxy-2-nitrobenzyl (DMNB) group into Ang-II resulted in a caged Ang-II analog that is effectively inactive towards both AT1R and AT2R and cell permeable but easily converted back to active Ang-II upon irradiation with UV. Using cAng-II to activate intracellular Ang-II receptors permits a comparison of the signalling events and physiological function associated with selective activation of either cell surface or intracellular Ang-II receptors. Although activation of intracellular ATRs had similar effects to extracellular Ang-II on the abundance of NK-κB mRNA and 18S rRNA, activation of nuclear ATRs induced a greater increase in on $[Ca^{2+}]_n$. Hence, physiological conditions that alter the production in iAng-II may have consequences that are distinct from changes in extracellular/circulating Ang-II. In addition, drugs may have unpredicted effects depending on whether they access only the cell surface receptors or are able to enter the cell and alter the function of intracellular receptors. Targeting drugs to either the cell surface receptor or the intracellular receptor may have therapeutically beneficial consequences.

Disclosure:

The authors declare no conflicts of interest.

Acknowledgments

The authors thank Nathalie L'Heureux and Chantal St-Cyr for technical assistance, and Dr. Feng Xiong for statistical analyses. Supported by grants from the Canadian Institutes for Health Research (CIHR: 6957 and 68929 to SN; 125970 to BGA), the Quebec Heart and Stroke Foundation, and the Fondation Leducq (ENAFRA Network, 07/CVD/03). AT was supported by an FRQS-RSCV/HSFQ doctoral scholarship.

Figure Legends

Figure 1. AT1R-dependent ERK1/2-phosphorylation following photolysis of cAng-II. P-ERK1/2 and ERK immunoreactivity in AT1R-transfected HEK 293 cells treated with vehicle (Ctl), in the presence or absence of 10-nM Ang-II or [Tyr(DMNB)^4]Ang-II (cAng-II), or valsartan (Val; 1 μM, 30 min) with or without UV-irradiation (UV; 1 min). Data shown is mean ± SEM of three independent determinations. ***$P < 0.001$, ns = non-significant. From Tadevosyan A *et al.*, (2015) Photoreleasable ligands to study intracrine angiotensin II signalling. J Physiol 593.3, 521-539. Reprinted with permission from John Wiley & Sons, Inc.

Figure 2. AT2R-dependent cGMP production following photolysis of cAng-II. cGMP was measured in serum-starved HEK 293 cells transfected with AT2R following incubation with vehicle (control), Ang-II (10 nM) or [Tyr(DMNB)^4]Ang-II (cAng-II, 10 nM), in the presence of PD123319 (PD, 1 μM), L-NAME (L-N, 1 mM), and UV-irradiation, as indicated. Data shown mean±SEM, n = 3/condition, ***$P < 0.001$, ##$P < 0.01$ or ###$P < 0.001$ vs. Ang-II, §§§$P < 0.001$ vs. cAng-II, ns = non-significant. From Tadevosyan A *et al.*, (2015) Photoreleasable ligands to study intracrine angiotensin II signalling. J Physiol 593.3, 521-539. Reprinted with permission from John Wiley & Sons, Inc.

Figure 3. Cellular uptake of fluorescein-cAng-II. Intracellular distribution of fluorescein-[Ahx^0]Ang-II, fluorescein-[Ahx^0,Tyr(DMNB)^4]Ang-II, fluorescein-[Ahx^0]PACAP(28-38) and fluorescein-[Ahx^0]TAT(48-60) upon confocal microscopy in live non-permeabilized HEK 293 cells. Cell Mask was used to delineate the plasma membrane and nuclei, respectively. Data shown is mean ± SEM, ***$P < 0.001$. From Tadevosyan A *et al.*, (2015) Photoreleasable ligands

to study intracrine angiotensin II signalling. J Physiol 593.3, 521-539. Reprinted with permission from John Wiley & Sons, Inc.

Figure 4. Response of nucleoplasmic and [Ca^{2+}] to activation of intracellular versus cell-surface angiotensin receptors. Nucleoplasmic [Ca^{2+}] recorded in canine cardiomyocytes before (t = 10 s) and 300 s after (t = 400 s) photolysis in cells loaded with vehicle (control), 20 nM cAng-II, 20 nM cAng-II + 1 μM valsartan, 20 nM cAng-II + 100 μM 2-APB, 1 μM valsartan alone or extracellularly administered 20 nM Ang-II with or without 1 μM Valsartan. Photolysis was induced by a pulse of UV-light (2-5 s, 70 μW) from a 405-nm/30-mW diode. DRAQ5 fluorescence was used to select the area corresponding to the nucleoplasm. Signals are presented as background-subtracted normalized fluorescence (%F/F_0), where F is the fluorescence intensity and F_0 is the resting fluorescence in the same cell prior to photolysis (t = 10 s). For each condition (n = 8-12 cells), mean nuclear Fluo-4 fluorescence at baseline (t = 10 s; hatched bars) or after stimulation (t = 400 s) was quantified. Data are mean ± SEM, ****P < 0.001, *****P < 0.0001 ns=nonsignificant*. From Tadevosyan A et al., (2015) Photoreleasable ligands to study intracrine angiotensin II signalling. J Physiol 593.3, 521-539. Reprinted with permission from John Wiley & Sons, Inc.

References

[1]. Vaniotis G, Allen BG, Hébert TE. Nuclear GPCRs in cardiomyocytes: an insider's view of β-adrenergic receptor signaling. Am J Physiol Heart Circ Physiol. 2011;301:H1754-H64.

[2]. Tadevosyan A, Vaniotis G, Allen BG, Hebert TE, Nattel S. G protein-coupled receptor signalling in the cardiac nuclear membrane: evidence and possible roles in physiological and pathophysiological function. J Physiol. 2012;590:1313-30.

[3]. Branco AF, Allen BG. G protein-coupled receptor signaling in cardiac nuclear membranes. Journal of Cardiovasc Pharmacol. 2015;65:101-9.

[4]. Lu D, Yang H, Shaw G, Raizada MK. Angiotensin II-induced nuclear targeting of the angiotensin type 1 (AT_1) receptor in brain neurons. Endocrinology. 1998;139:365-75.

[5]. Gobeil F, Jr., Dumont I, Marrache AM, Vazquez-Tello A, Bernier SG, Abran D, et al. Regulation of eNOS expression in brain endothelial cells by perinuclear EP_3 receptors. Circ Res. 2002;90:682-9.

[6]. Wright CD, Chen Q, Baye NL, Huang Y, Healy CL, Kasinathan S, et al. Nuclear α1-adrenergic receptors signal activated ERK localization to caveolae in adult cardiac myocytes. Circ Res. 2008;103:992-1000.

[7]. Ryall KA, Saucerman JJ. Automated imaging reveals a concentration dependent delay in reversibility of cardiac myocyte hypertrophy. J Mol Cell Cardiol. 2012;53:282-90.

[8]. Wright CD, Wu SC, Dahl EF, Sazama AJ, O'Connell TD. Nuclear localization drives α1-adrenergic receptor oligomerization and signaling in cardiac myocytes. Cell Signal. 2012;24:794-802.

[9]. Wu SC, Dahl EF, Wright CD, Cypher AL, Healy CL, O'Connell TD. Nuclear localization of α1A-adrenergic receptors is required for signaling in cardiac myocytes: an "inside-out" α1-AR signaling pathway. J Am Heart Assoc. 2014;3:e000145.

[10]. Buu NT, Hui R, Falardeau P. Norepinephrine in neonatal rat ventricular myocytes: association with the cell nucleus and binding to nuclear alpha 1- and beta-adrenergic receptors. J Mol Cell Cardiol. 1993;25:1037-46.

[11]. Merlen C, Ledoux J. Single-cell microinjection coupled to confocal microscopy to characterize nuclear membrane receptors in freshly isolated cardiomyocytes. In: Allen BG, Hébert TE, editors. Nuclear G Protein-Coupled Receptors: Methods and Protocols. New York: Springer New York; 2015. p. 9-16.

[12]. Chatenet D, Bourgault S, Fournier A. Design and application of light-activated probes for cellular signaling. In: Allen BG, Hébert TE, editors. Nuclear G Protein-Coupled Receptors: Methods and Protocols. New York: Springer New York; 2015. p. 17-30.

[13]. McCray JA, Herbette L, Kihara T, Trentham DR. A new approach to time-resolved studies of ATP-requiring biological systems; laser flash photolysis of caged ATP. Proc Natl Acad Sci U S A. 1980;77:7237-41.

[14]. Schlichting I, Rapp G, John J, Wittinghofer A, Pai EF, Goody RS. Biochemical and crystallographic characterization of a complex of c-Ha-ras p21 and caged GTP with flash photolysis. Proc Natl Acad Sci U S A. 1989;86:7687-90.

[15]. Bourgault S, Létourneau M, Fournier A. Development of photolabile caged analogs of endothelin-1. Peptides. 2007;28:1074-82.

[16]. Merlen C, Farhat N, Luo X, Chatenet D, Tadevosyan A, Villeneuve LR, et al. Intracrine endothelin signaling evokes IP3-dependent increases in nucleoplasmic Ca^{2+} in adult cardiac myocytes. J Mol Cell Cardiol. 2013;62:189-202.

[17]. Muralidharan S, Nerbonne JM. Photolabile "caged" adrenergic receptor agonists and related model compounds. J Photochem Photobiol B. 1995;27:123-37.

[18]. Vaniotis G, Glazkova I, Merlen C, Smith C, Villeneuve LR, Chatenet D, et al. Regulation of cardiac nitric oxide signalling by nuclear β-adrenergic and endothelin receptors. J Mol Cell Cardiol. 2013;62:58-68.

[19]. Muralidharan S, Maher GM, Boyle WA, Nerbonne JM. "Caged" phenylephrine: development and application to probe the mechanism of alpha-receptor-mediated vasoconstriction. Proc Natl Acad Sci U S A. 1993;90:5199-203.

[20]. Wang SS, Augustine GJ. Confocal imaging and local photolysis of caged compounds: dual probes of synaptic function. Neuron. 1995;15:755-60.

[21]. Bourgault S, Letourneau M, Fournier A. Development and pharmacological characterization of "caged" urotensin II analogs. Peptides. 2005;26:1475-80.

[22]. Tertyshnikova S, Fein A. Inhibition of inositol 1,4,5-trisphosphate-induced Ca^{2+} release by cAMP-dependent protein kinase in a living cell. Proc Natl Acad Sci U S A. 1998;95:1613-7.

[23]. Li W, Llopis J, Whitney M, Zlokarnik G, Tsien RY. Cell-permeant caged $InsP_3$ ester shows that Ca^{2+} spike frequency can optimize gene expression. Nature (London). 1998;392:936-41.

[24]. Ghosh M, Song X, Mouneimne G, Sidani M, Lawrence DS, Condeelis JS. Cofilin promotes actin polymerization and defines the direction of cell motility. Science. 2004;304:743-6.

[25]. Monroe WT, McQuain MM, Chang MS, Alexander JS, Haselton FR. Targeting expression with light using caged DNA. J Biol Chem. 1999;274:20895-900.

[26]. Chaulk SG, MacMillan AM. Caged RNA: photo-control of a ribozyme reaction. Nucleic Acids Res. 1998;26:3173-8.

[27]. Ando H, Furuta T, Tsien RY, Okamoto H. Photo-mediated gene activation using caged RNA/DNA in zebrafish embryos. Nat Genet. 2001;28:317-25.

[28]. Tadevosyan A, Letourneau M, Folch B, Doucet N, Villeneuve LR, Mamarbachi AM, et al. Photoreleasable ligands to study intracrine angiotensin II signalling. J Physiol. 2015;593:521-39.

[29]. Zhang X, Wang G, Dupre DJ, Feng Y, Robitaille M, Lazartigues E, et al. Rab1 GTPase and dimerization in the cell surface expression of angiotensin II type 2 receptor. J Pharmacol Exp Ther. 2009;330:109-17.

[30]. Tadevosyan A, Allen BG, Nattel S. Isolation and study of cardiac nuclei from canine myocardium and adult ventricular myocytes. In: Allen BG, Hébert TE, editors. Nuclear G Protein-Coupled Receptors: Methods and Protocols. New York: Springer New York; 2015. p. 69-80.

[31]. Doan ND, Letourneau M, Vaudry D, Doucet N, Folch B, Vaudry H, et al. Design and characterization of novel cell-penetrating peptides from pituitary adenylate cyclase-activating polypeptide. J Control Release. 2012;163:256-65.

[32]. Tadevosyan A, Maguy A, Villeneuve LR, Babin J, Bonnefoy A, Allen BG, et al. Nuclear-delimited angiotensin receptor-mediated signaling regulates cardiomyocyte gene expression. J Biol Chem. 2010;295:22338-49.

[33]. Morinelli TA, Raymond JR, Baldys A, Yang Q, Lee MH, Luttrell L, et al. Identification of a putative nuclear localization sequence within ANG II AT_{1A} receptor associated with nuclear activation. Am J Physiol Cell Physiol. 2007;292:C1398-C408.

[34]. Malhotra R, Sadoshima J, Brosius FC, 3rd, Izumo S. Mechanical stretch and angiotensin II differentially upregulate the renin-angiotensin system in cardiac myocytes In vitro. Circ Res. 1999;85:137-46.

[35]. Tsai CT, Lai LP, Hwang JJ, Chen WP, Chiang FT, Hsu KL, et al. Renin-angiotensin system component expression in the HL-1 atrial cell line and in a pig model of atrial fibrillation. Journal of Hypertension. 2008;26:570-82.

[36]. Clausmeyer S, Reinecke A, Farrenkopf R, Unger T, Peters J. Tissue-specific expression of a rat renin transcript lacking the coding sequence for the prefragment and its stimulation by myocardial infarction. Endocrinology. 2000;141:2963-70.

[37]. Frustaci A, Kajstura J, Chimenti C, Jakoniuk I, Leri A, Maseri A, et al. Myocardial cell death in human diabetes. Circ Res. 2000;87:1123-32.

[38]. Singh VP, Le B, Bhat VB, Baker KM, Kumar R. High-glucose-induced regulation of intracellular ANG II synthesis and nuclear redistribution in cardiac myocytes. Am J Physiol. 2007;293:H939-48.

[39]. Fiordaliso F, Leri A, Cesselli D, Limana F, Safai B, Nadal-Ginard B, et al. Hyperglycemia activates p53 and p53-regulated genes leading to myocyte cell death. Diabetes. 2001;50:2363-75.

[40]. Singh VP, Baker KM, Kumar R. Activation of the intracellular renin-angiotensin system in cardiac fibroblasts by high glucose: role in extracellular matrix production. Am J Physiol. 2008;294:H1675-84.

[41]. Lavrentyev EN, Estes AM, Malik KU. Mechanism of high glucose induced angiotensin II production in rat vascular smooth muscle cells. Circ Res. 2007;101:455-64.

[42]. Vidotti DB, Casarini DE, Cristovam PC, Leite CA, Schor N, Boim MA. High glucose concentration stimulates intracellular renin activity and angiotensin II generation in rat mesangial cells. Am J Physiol. 2004;286:F1039-F45.

[43]. Baker KM, Chernin MI, Schreiber T, Sanghi S, Haiderzaidi S, Booz GW, et al. Evidence of a novel intracrine mechanism in angiotensin II-induced cardiac hypertrophy. Regul Pept. 2004;120:5-13.

[44]. Mazzolai L, Nussberger J, Aubert JF, Brunner DB, Gabbiani G, Brunner HR, et al. Blood pressure-independent cardiac hypertrophy induced by locally activated renin-angiotensin system. Hypertension. 1998;31:1324-30.

[45]. Dostal DE, Rothblum KN, Conrad KM, Cooper GR, Baker KM. Detection of angiotensin I and II in cultured rat cardiac myocytes and fibroblasts. Am J Physiol. 1992;263:C851-C63.

[46]. Camargo de Andrade MC, Di Marco GS, de Paulo Castro Teixeira V, Mortara RA, Sabatini RA, Pesquero JB, et al. Expression and localization of N-domain ANG I-converting enzymes in mesangial cells in culture from spontaneously hypertensive rats. Am J Physiol Renal Physiol. 2006;290:F364-75.

Figure 1

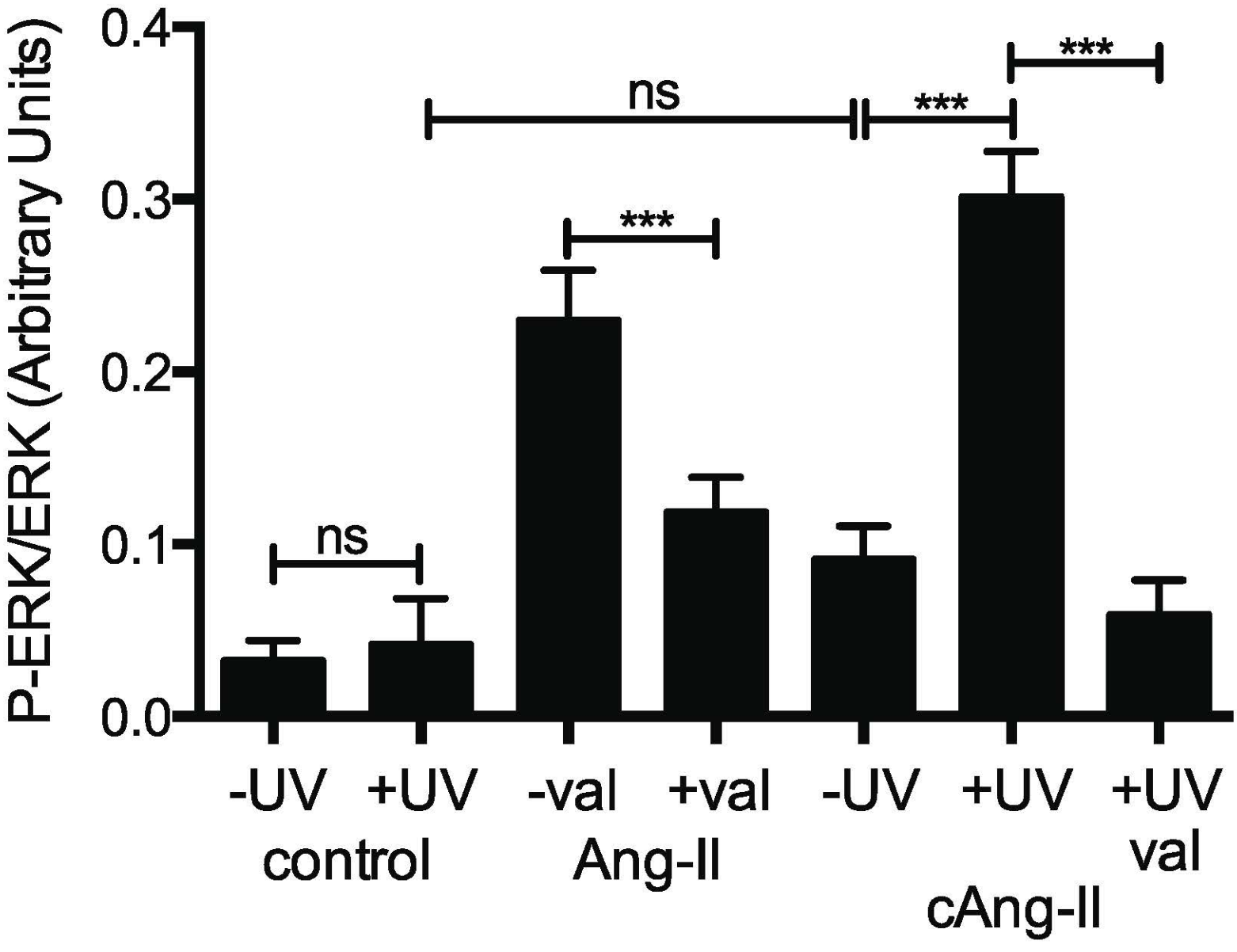
P-ERK/ERK (Arbitrary Units)
0.4
0.3
0.2
0.1
0.0
ns
***
***
***
ns
-UV
+UV
-val
+val
-UV
+UV
+UV
control
Ang-II
cAng-II
val

Figure 2

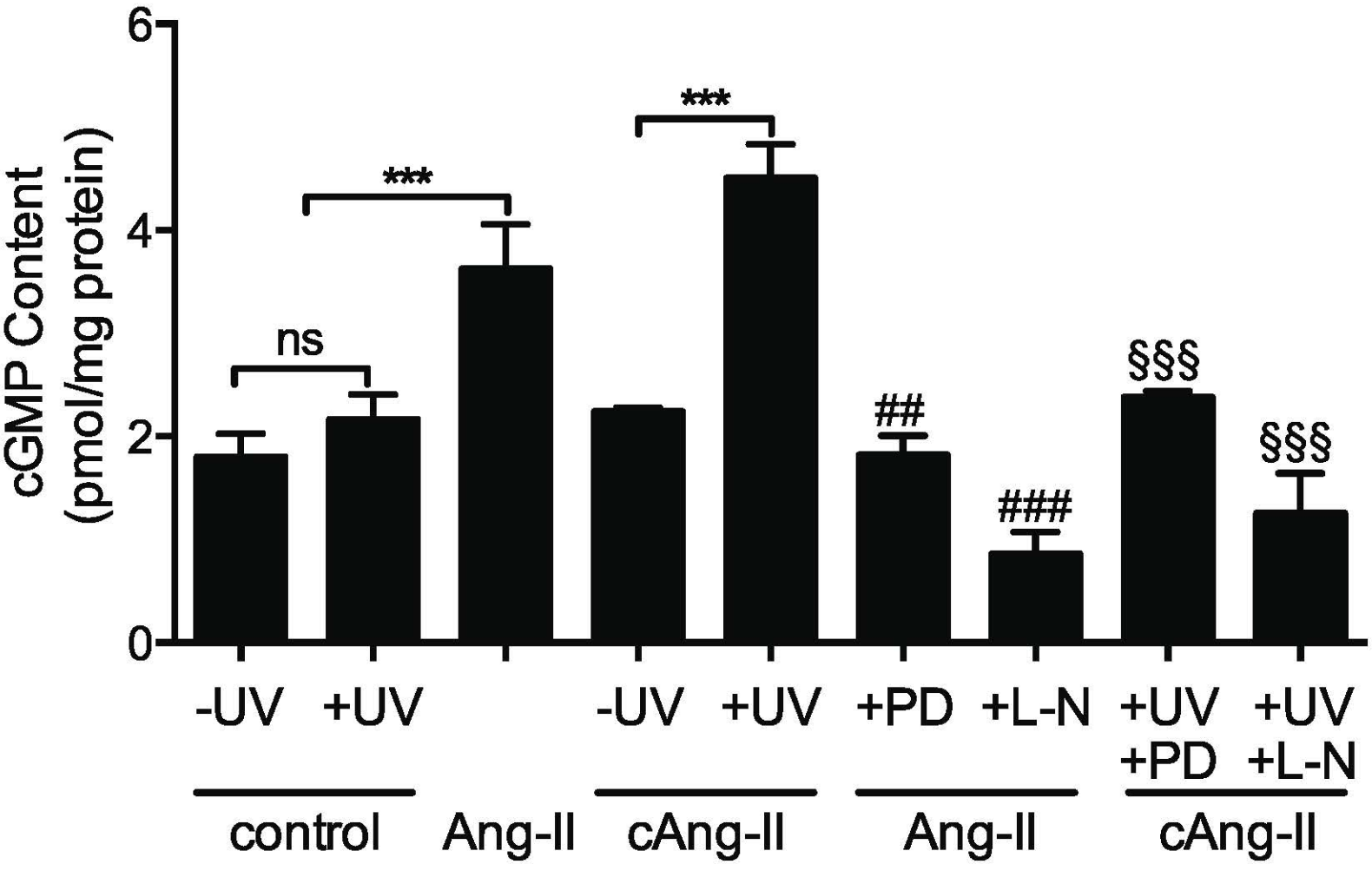
cGMP Content
(pmol/mg protein)
6
4
2
0
ns
***
***
##
###
§§§
§§§
-UV
+UV
-UV
+UV
+PD
+L-N
+UV
+PD
+UV
+L-N
control
Ang-II
cAng-II
Ang-II
cAng-II

Figure 3

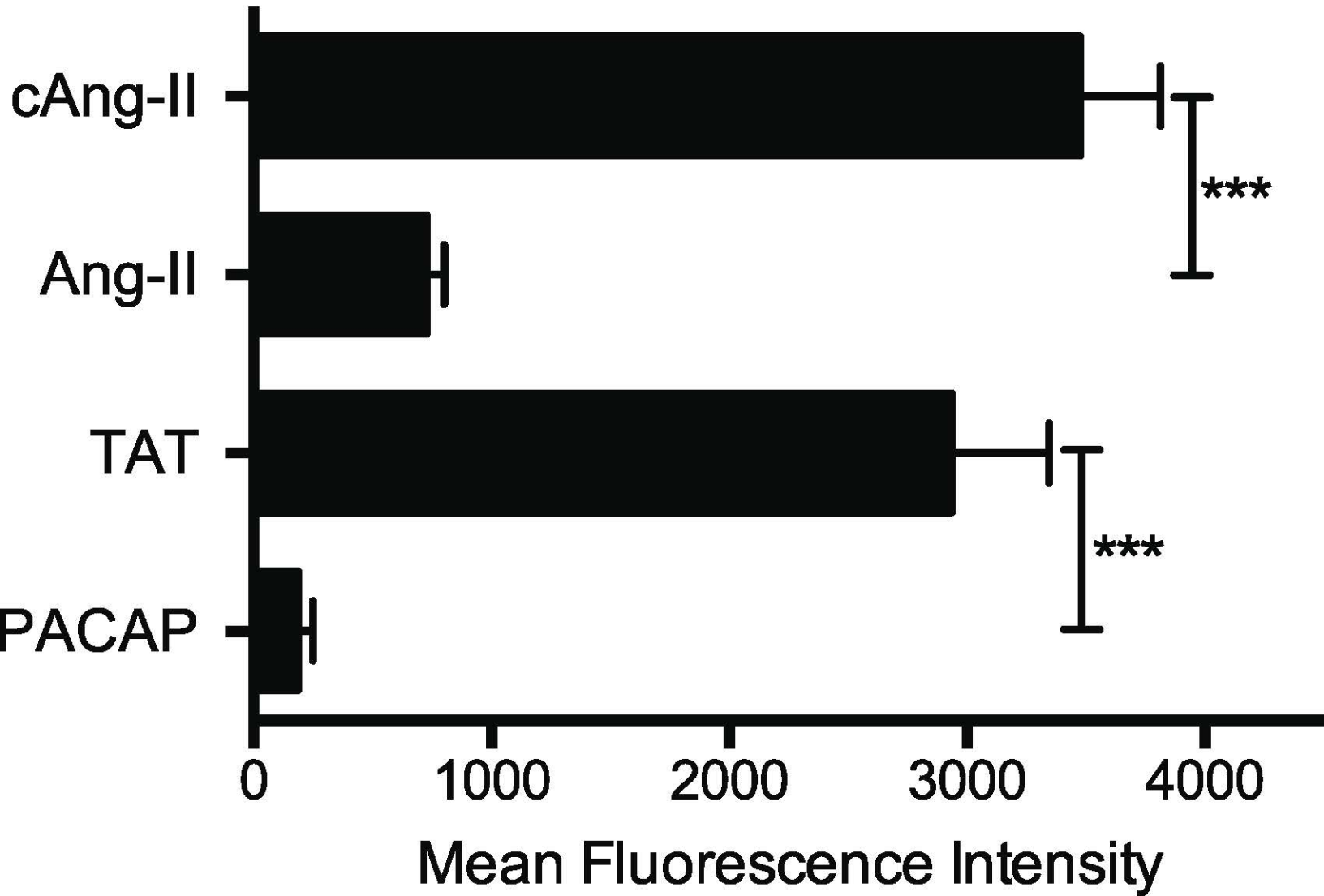
cAng-II
Ang-II
TAT
PACAP
***
***
0
1000
2000
3000
4000
Mean Fluorescence Intensity

Figure 4

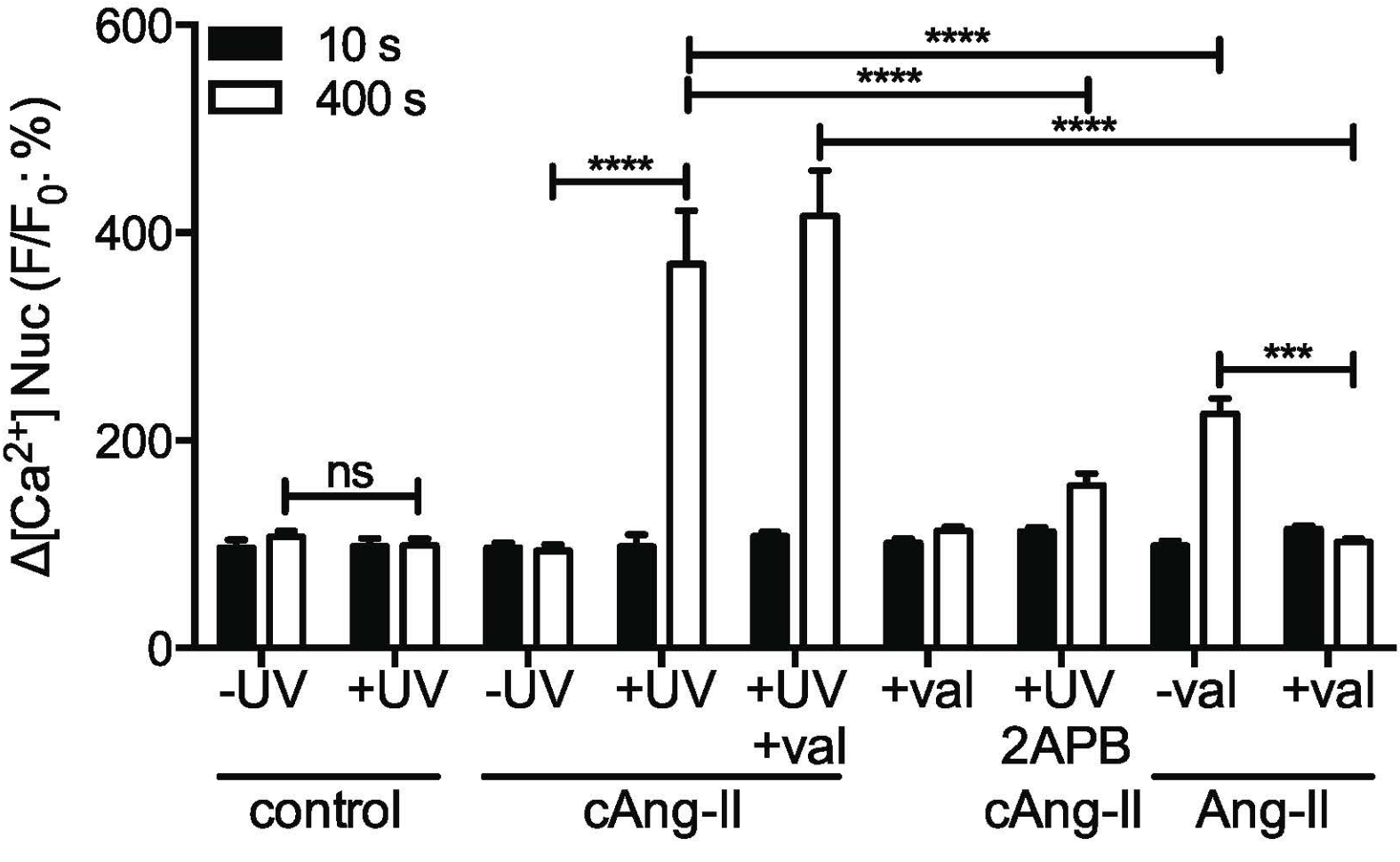
600
400
200
0
10 s
400 s
Δ[Ca2+] Nuc (F/F0: %)
ns
****
****
****
****
***
-UV
+UV
-UV
+UV
+UV +val
+val
+UV 2APB cAng-II
-val
+val
control
cAng-II
Ang-II

Table 1

Table 1. Effect of ligand permability upon nuclear GPCR function.

ligand	Nuclear receptor has no function	Nuclear receptor has same function as cell surface receptor	Nuclear receptor has a unique function
Impermeable	N	N	N
Permeable	N	E	U
Caged pro-drug	N	S	U

N, no effect; E, enhanced effect compared to activation of cell suface receptor alone; S, same effect as activation of cell surface receptor alone; U, unique effect compared to activation of cell suface receptor.